

RESEARCH

Open Access



Can intraoperative improvement of radial endobronchial ultrasound imaging enhance the diagnostic yield in peripheral pulmonary lesions?

Kazuki Nishida^{1,2}, Takayasu Ito^{3*}, Shingo Iwano⁴, Shotaro Okachi⁵, Shota Nakamura⁶, Basile Chrétien^{1,7}, Toyofumi Fengshi Chen-Yoshikawa⁶ and Makoto Ishii³

Abstract

Background Data regarding the diagnostic efficacy of radial endobronchial ultrasound (R-EBUS) findings obtained via transbronchial needle aspiration (TBNA)/biopsy (TBB) with endobronchial ultrasonography with a guide sheath (EBUS-GS) for peripheral pulmonary lesions (PPLs) are lacking. We evaluated whether intraoperative probe repositioning improves R-EBUS imaging and affects diagnostic yield and safety of EBUS-guided sampling for PPLs.

Methods We retrospectively studied 363 patients with PPLs who underwent TBNA/TBB (83 lesions) or TBB (280 lesions) using EBUS-GS. Based on the R-EBUS findings before and after these procedures, patients were categorized into three groups: the improved R-EBUS image ($n=52$), unimproved R-EBUS image ($n=69$), and initial within-lesion groups ($n=242$). The impact of improved R-EBUS findings on diagnostic yield and complications was assessed using multivariable logistic regression, adjusting for lesion size, lesion location, and the presence of a bronchus leading to the lesion on CT. A separate exploratory random-forest model with SHAP analysis was used to explore factors associated with successful repositioning in lesions not initially “within.”

Results The diagnostic yield in the improved R-EBUS group was significantly higher than that in the unimproved R-EBUS group (76.9% vs. 46.4%, $p=0.001$). The regression model revealed that the improvement in intraoperative R-EBUS findings was associated with a high diagnostic yield (odds ratio: 3.55, 95% confidence interval, 1.57–8.06, $p=0.002$). Machine learning analysis indicated that inner lesion location and radiographic visibility were the most influential predictors of successful repositioning. The complication rates were similar across all groups (total complications: 5.8% vs. 4.3% vs. 6.2%, $p=0.943$).

Conclusions Improved R-EBUS findings during TBNA/TBB or TBB with EBUS-GS were associated with a high diagnostic yield without an increase in complications, even when the initial R-EBUS findings were inadequate. This suggests that repeated intraoperative probe repositioning can safely boost outcomes.

*Correspondence:
Takayasu Ito
takaito9@med.nagoya-u.ac.jp

Full list of author information is available at the end of the article



© The Author(s) 2025. **Open Access** This article is licensed under a Creative Commons Attribution-NonCommercial-NoDerivatives 4.0 International License, which permits any non-commercial use, sharing, distribution and reproduction in any medium or format, as long as you give appropriate credit to the original author(s) and the source, provide a link to the Creative Commons licence, and indicate if you modified the licensed material. You do not have permission under this licence to share adapted material derived from this article or parts of it. The images or other third party material in this article are included in the article's Creative Commons licence, unless indicated otherwise in a credit line to the material. If material is not included in the article's Creative Commons licence and your intended use is not permitted by statutory regulation or exceeds the permitted use, you will need to obtain permission directly from the copyright holder. To view a copy of this licence, visit <http://creativecommons.org/licenses/by-nc-nd/4.0/>.

Keywords Radial endobronchial ultrasound imaging, Diagnostic yield, Peripheral pulmonary lesions, Intraoperative repositioning, Endobronchial ultrasound-guided biopsy, Transbronchial needle aspiration, Transbronchial biopsy

Background

The widespread use of low-dose computed tomography (CT) has contributed to the early detection of lung cancer and reduced mortality [1]. Although the detection of peripheral pulmonary lesions (PPLs), including small lesions, has increased with low-dose CT screening, making a definitive diagnosis solely through imaging is difficult. Thus, tissue retrieval is crucial for determining treatment strategies for PPLs.

Surgical lung biopsy (SLB), transthoracic needle biopsy (TTNB), and bronchoscopy are common modalities for tissue retrieval [2]. Bronchoscopy is often preferred as the initial procedure because it has fewer complications than those of SLB or TTNB. Conventional bronchoscopy with fluoroscopy has a diagnostic yield of only around 30–60%, which is inadequate compared with the approximately 90% yield of SLB and TTNB [3]. Recent advances in image-guided bronchoscopy, particularly the integration of radial endobronchial ultrasound (R-EBUS) with navigation systems, such as virtual bronchoscopic navigation and electromagnetic navigation, have increased the diagnostic yield of PPLs to approximately 70% [4, 5]. Furthermore, systematic reviews and meta-analyses have refined these estimates, reporting a pooled diagnostic yield of approximately 72% (95% confidence interval [CI]: 70–75%) for R-EBUS-guided transbronchial biopsy [6].

Diagnostic success is strongly influenced by the positional relation between the ultrasound probe and lesion. Yamada et al. reported a diagnostic yield of 83% when the probe was positioned within the lesion, 61% when merely adjacent, and only 4% when located outside [7]. Similar findings have been reported, underscoring the critical importance of achieving an intralesional probe position [6, 8]. While Guvenc et al. [9] demonstrated that CT characteristics significantly influenced the success rate of R-EBUS-guided diagnosis of pulmonary lesions, Ali et al. [4] further confirmed through systematic review and meta-analysis that lesion size and the presence of a bronchus leading to the lesion strongly affected the diagnostic yield of R-EBUS for patients with PPLs. These findings collectively indicate that although securing a ‘within’ position is key to maximizing the diagnostic yield, inherent anatomical complexities and technical constraints often prevent its consistent achievement in all PPLs.

Transbronchial needle aspiration (TBNA) with EBUS-GS, when performed with the probe positioned adjacent to or away from the lesion, has been reported to improve the probe–lesion relation and facilitate repeated sampling through the guide sheath, thereby increasing the diagnostic yield [10, 11]. However, the quantitative impact of

repeated intraoperative efforts, such as achieving deeper probe penetration during transbronchial biopsy to refine probe positioning, remains unproven. Therefore, this study aimed to evaluate whether such intraoperative improvements could significantly enhance the diagnostic yield without increasing the complication rate.

Methods

Study design

A retrospective analysis was performed on consecutive patients with PPLs who underwent TBB and TBNA via EBUS-GS at Nagoya University Hospital between April 1, 2019, and March 31, 2022. Patients with bronchial lumen lesions or unknown final diagnoses were excluded to maintain focus on peripheral lesions and eliminate diagnostic uncertainty. An overview of this selection process is presented in Fig. 1. Our study design and sampling protocol were developed in accordance with the methodological framework described by Ito et al., which specifically focused on evaluating the diagnostic value and safety of adding TBNA to TBB using EBUS-GS [12]. This study was conducted in accordance with the STROBE guidelines.

Bronchoscopic procedures

Prior to bronchoscopy, all participants received pharyngeal anaesthesia using a 1% lidocaine spray and intravenous anaesthesia with midazolam, fentanyl, or pentazocine. All procedures were performed under the direct supervision of pulmonologists with extensive experience in radial-EBUS-guided TBNA/TBB at our institution. Bronchoscopy was initiated using a thin GS (K-201; Olympus; 1.95 mm outer diameter) coated with a 20 MHz radial ultrasound probe (UM-S20-17 S; Olympus, diameter 1.4 mm) and thin bronchoscope (BF-P260F; Olympus, Tokyo, Japan). A convex-probe EBUS bronchoscope was not used in any case. In all cases, the bronchoscope was carefully inserted into the nearest affected bronchus leading to the lesion using a virtual bronchoscopic navigation generated on a workstation (SYNAPSE VINCENT version 4.0, Fuji Medical Systems, Tokyo, Japan). An ultrasound probe was then inserted into the target bronchus to reach the lesion, and the R-EBUS images were confirmed. At this point, the probe's position relative to the lesion was categorized as either within (completely encompassed by the lesion), adjacent (in contact with the lesion), or invisible (away from the lesion). After the initial R-EBUS image was obtained, the attending pulmonologist decided whether to add TBNA. TBNA was omitted when the probe lay within the lesion

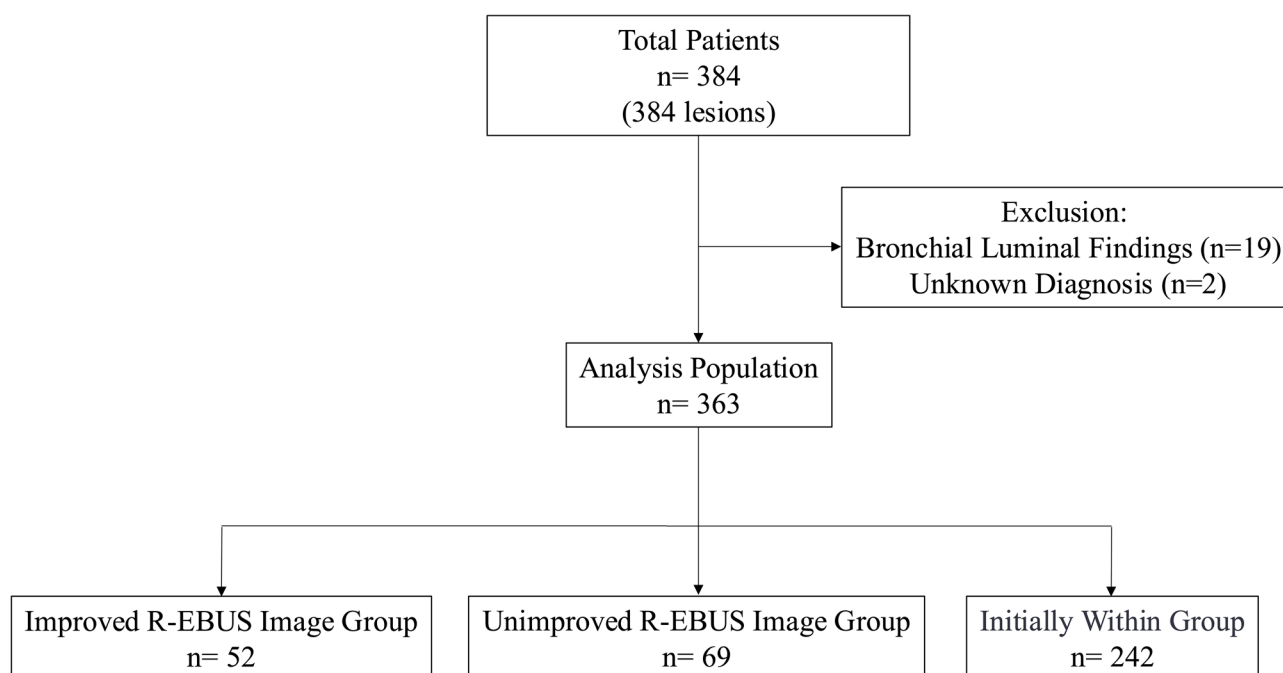


Fig. 1 Study flow diagram. A flow diagram illustrating the patient selection process. A total of 384 patients with peripheral pulmonary lesions (PPLs) underwent transbronchial needle aspiration (TBNA) and/or transbronchial biopsy (TBB) using endobronchial ultrasonography with a guide sheath (EBUS-GS) between April 2019 and March 2022. After excluding 19 patients with bronchial luminal findings and two patients with unknown final diagnoses, the remaining 363 eligible patients were divided into three groups: improved R-EBUS imaging group ($n=52$), unimproved R-EBUS imaging group ($n=69$), and initially within-group ($n=242$)

and the guide sheath could be re-introduced to the same position with confidence. TBNA was added when the initial image was adjacent or invisible, or when the probe was within the lesion but reproducible access could not be assured, in order to create a stable tract before forceps biopsy. After initial image acquisition, if the probe was within the lesion, no further repositioning was performed. However, if the probe was not within the lesion, repositioning was undertaken to improve R-EBUS imaging. In such cases, additional maneuvers included adjusting the bronchoscope up and down as well as employing rotational movements. Notably, because the flexible bronchoscope was originally designed for left-handed operation by Dr. Ikeda, switching it to right-hand use maximizes the available counterclockwise rotation. This technical modification was recently reported as effective by Shinagawa's group in Hokkaido [13]. Once the final R-EBUS position was confirmed, the probe was removed, and TBNA was performed using a 21-gauge needle (PeriView Flex, Olympus) through the thin GS with a back-and-forth motion applied at least twice for each lesion. After each TBNA pass, the radial probe was re-introduced through the guide sheath to obtain a final R-EBUS image; this post-TBNA image (within, adjacent, or invisible) was used to categorise lesions as 'improved' or 'unimproved'. This was followed by TBB via EBUS-GS using forceps biopsy (FB-233D; Olympus) at least nine

times for every lesion under fluoroscopic guidance. In some cases, TBB via EBUS-GS was performed as a stand-alone procedure without TBNA, or after completing TBNA. Figure 2 illustrates representative R-EBUS images for these categories (Fig. 2a: within; Fig. 2b: adjacent; Fig. 2c: invisible), following the protocol outlined by Ito et al., which emphasized the added value of combining sampling techniques [12].

Variables

The primary outcome of this study was the diagnostic yield of TBNA followed by TBB (TBNA/TBB) or TBB alone via EBUS-GS. The diagnostic yield was defined as the proportion of patients in whom TBNA/TBB or TBB via EBUS-GS provided a definitive final diagnosis of PPLs. The final diagnosis was confirmed based on the pathological findings of biopsy specimens from bronchoscopy, TTNB, and SLB. When the collected specimens demonstrated malignancy (i.e., specific findings on histology or positive cytology) consistent with the final diagnosis, bronchoscopy was considered diagnostic. When the collected specimens demonstrated specific benign findings (such as granuloma or organizing pneumonitis) and the subsequent clinical course showed radiological improvement and lesion stability for >6 months after the procedure, bronchoscopy was considered diagnostic [14]. However, when samples were inadequate (including

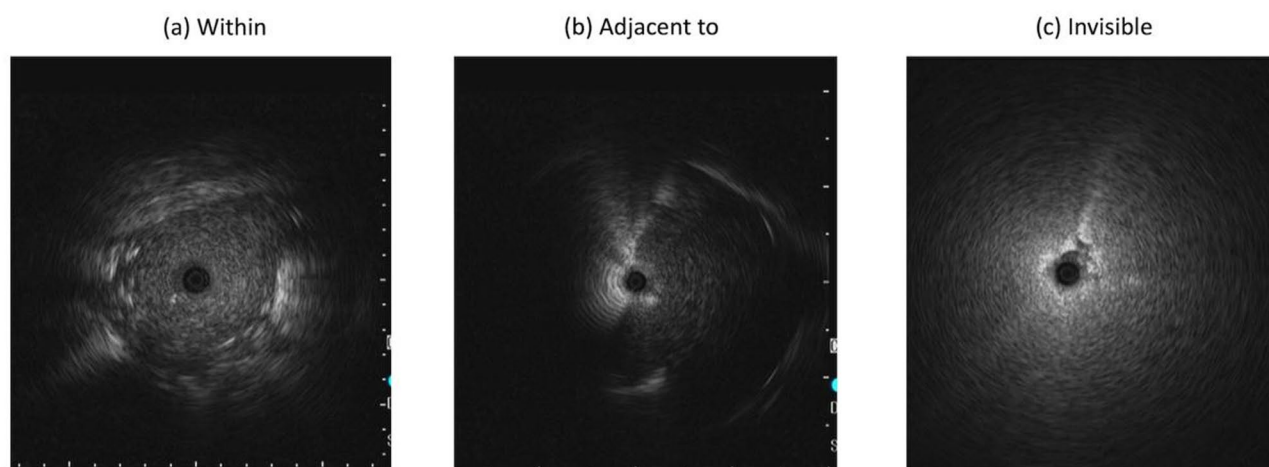


Fig. 2 Representative radial endobronchial ultrasound (R-EBUS) images based on probe–lesion relation. R-EBUS images showing the three positional categories based on the relation between the ultrasound probe and peripheral pulmonary lesions: **(a)** “Within” – The probe is positioned inside the lesion, completely surrounded by the lesion; **(b)** “Adjacent to” – The probe is in contact with the lesion, partially surrounded by the lesion; **(c)** “Invisible” – The probe is away from the lesion, showing minimal or no visualization of the lesion margin. These classifications were used to determine whether intraoperative improvements in R-EBUS findings (from “invisible” to “adjacent” or “within,” or from “adjacent” to “within”) affected diagnostic yield. All the images were acquired with the 20 MHz radial-probe EBUS described in the Methods section

peripheral lung and peribronchial tissues), bronchoscopy was classified as a failed diagnosis. Procedure duration was not collected because start- and finish-time stamps were not recorded in the electronic bronchoscopy log.

The main explanatory variable was defined as an improvement in the relation between the probe and lesion. The R-EBUS image was classified as improved when the probe–lesion positional relation changed from invisible to adjacent or within, or from adjacent to within. When the probe–lesion positional relation remained either invisible or adjacent, it was classified as unimproved. If the probe–lesion positional relation was initially within, improvement was not evaluated. The analysis population was divided into three groups according to the R-EBUS image: initially within group: probe initially positioned within the lesion, improved R-EBUS image group: probe initially not within the lesion whose R-EBUS category shifted upward, and unimproved R-EBUS image group: probe initially not within the lesion and whose category did not change.

Other variables were collected to obtain patient backgrounds and clinical characteristics. Lesion location relative to the hilum was classified as follows: inner: lesions within the inner and middle third ellipses, and outer: lesions within the outer third ellipse [15]. Lesion structures were classified into two categories: solid and sub-solid [16]. Complications during bronchoscopy were classified according to previous reports [17]. In this study, the definitions of complications were as follows: pneumothorax: any case requiring chest drainage; infection: development of new pneumonia and/or pleuritis or worsening of pre-existing pleurisy after the procedure; haemorrhage: blood loss of ≥ 300 mL or any bleeding

necessitating a blood transfusion or haemostatic intervention; other complications: any adverse events not classified as pneumothorax, infection, or haemorrhage; and total complications: overall incidence of all recorded events.

Statistical analysis

To summarize the patient characteristics, categorical variables are presented as frequencies and percentages, whereas continuous variables are presented as medians and interquartile ranges. Differences between the improved and unimproved R-EBUS image groups were compared using the Mann–Whitney U test for continuous variables and Fisher’s exact test for categorical variables. The diagnostic yields of the improved R-EBUS image, unimproved R-EBUS image, and initially within-groups were compared using Fisher’s exact test for each pair of groups. As the main analysis, the impact of improved R-EBUS findings on diagnostic yield was evaluated using logistic regression analysis of the improved and unimproved R-EBUS image groups, adjusted for lesion size (dichotomized at 20 mm), lesion location from the hilum, and bronchus sign on CT. In a post-hoc subset restricted to lesions with a final malignant diagnosis, sensitivity for cancer was calculated and compared between groups with Fisher’s exact test. An exploratory logistic model with the same covariates was also fitted. Diagnostic yield was further compared between TBB-only and combined TBNA + TBB—both in the overall cohort and in lesions whose initial image was adjacent—again using Fisher’s exact test.

As a separate exploratory step, a random forest model was constructed in patients whose initial REBUS images

were not “within” (i.e., those eligible for repositioning), with the outcome defined as improved probe–lesion positioning. Predictors included lesion structure (solid versus subsolid), CT bronchus sign, radiographic visibility, continuous lesion size, and lesion location. A SHAP (SHapley Additive exPlanations) beeswarm plot was generated to visualize the non-linear and heterogeneous effects of these factors, thereby clarifying the clinical conditions associated with successful repositioning [18–20]. Complications among the three groups were compared using Fisher’s exact test. All data were complete with no missing values; therefore, no imputation was performed. In general, percentages are rounded to one decimal place, odds ratios (ORs) to two decimal places, and *p*-values to three decimal places. Statistical significance was set at *p* < 0.05. All statistical analyses were performed using R version 4.2.0 (R Foundation for Statistical Computing, Vienna, Austria).

Results

Study flow and patient characteristics

During the study period, 384 patients, each presenting with a single peripheral pulmonary lesion, underwent TBNA/TBB or TBB via EBUS-GS for PPLs. Among the 384 lesions, 19 patients with bronchial luminal findings and two patients with an unknown final diagnosis were excluded from the analysis. The remaining patients were divided into three groups: the improved R-EBUS image, unimproved R-EBUS image, and initially within-groups, which included 52, 69, and 242 patients, respectively (Fig. 1).

As shown in Table 1, the three groups were broadly similar in age, sex, lobar distribution, lesion texture, and CT bronchus sign. Median age was 72.5 years (IQR 66.8–77.3) in the improved group, 73.0 years (66.0–78.0) in the unimproved group, and 74.0 years (67.0–78.0) in the initial-within group. Male proportions were 71.2%, 56.5%, and 63.6% in the improved, unimproved, and initial-within cohorts, respectively. Inner-zone lesions were more frequent in the improved than in the unimproved group (55.8% vs. 36.2%, *p* = 0.042), whereas the initial-within cohort showed an intermediate frequency (50.4%). By design, almost all lesions in the improved and unimproved cohorts were initially “adjacent” on radial EBUS (96.2% and 84.1%, respectively). The prevalence of malignancy was 92.3% in the improved group, 76.8% in the unimproved group, and 83.5% in the initial-within group.

Diagnostic yield

Across all lesions, diagnostic yield varied according to both the initial REBUS category and the success of probe repositioning (Table 2). When the probe was initially within the lesion, yield was 82.2 % (199 / 242). Among lesions that were not initially within (*n* = 121), yield rose from 46.4 % (32 / 69) in the unimproved cohort to 76.9 % (40 / 52) in the improved cohort (*p* = 0.001). For lesions initially categorised as adjacent (*n* = 108), yield increased from 53.5 % (31 / 58) to 76.0 % (38 / 50) after successful repositioning (*p* = 0.017). For lesions with an invisible initial image (*n* = 13), yield climbed from 9.1 % (1 / 11) to 100% (2 / 2) when the probe could be repositioned into or adjacent to the lesion (*p* = 0.038).

Table 1 Characteristics of patients with peripheral pulmonary lesions by R-EBUS image improvement status

	Initial Adjacent or Invisible		<i>p</i>	Initial Within (<i>n</i> = 242)
	Improved EBUS Image Group (<i>n</i> = 52)	Unimproved EBUS Image Group (<i>n</i> = 69)		
Sex, male (%)	37 (71.2)	39 (56.5)	0.129	154 (63.6)
Age (median [IQR])	72.50 [66.75, 77.25]	73.00 [66.00, 78.00]	0.883	74.00 [67.00, 78.00]
Lobe (%)			> 0.999	
RUL + LUS	25 (48.1)	33 (47.8)		112 (46.3)
RML + lingula	7 (13.5)	10 (14.5)		27 (11.2)
RLL + LLL	20 (38.5)	26 (37.7)		103 (42.6)
Location, inner (%)	29 (55.8)	25 (36.2)	0.042	122 (50.4)
Texture, solid (%)	45 (86.5)	60 (87.0)	> 0.999	191 (78.9)
Bronchus sign, positive (%)	37 (71.2)	47 (68.1)	0.842	226 (93.4)
Size (median [IQR])	21.20 [15.01, 23.77]	19.30 [14.30, 24.51]	0.745	30.76 [23.00, 42.92]
Size, > 20 mm (%)	30 (57.7)	31 (44.9)	0.200	201 (83.1)
Visibility on radiograph, visible (%)	45 (86.5)	51 (73.9)	0.114	220 (90.9)
Initial EBUS image, adjacent to (%)	50 (96.2)	58 (84.1)	0.040	-
Initial EBUS image, invisible (%)	2 (3.8)	11 (15.9)	0.040	-
Malignancy (%)	48 (92.3)	53 (76.8)	0.027	202 (83.5)
Occurrence of Complications (%)	3 (5.8)	3 (4.3)	> 0.999	15 (6.2)
Diagnostic yield, positive (%)	40 (76.9)	32 (46.4)	0.001	199 (82.2)

EBUS, endobronchial ultrasound; IQR, interquartile range; RUL, right upper lobe; LUS, left upper segment; RML, right middle lobe; lingula, left lingula; RLL, right lower lobe; LLL, left lower lobe

Table 2 Diagnostic yield by initial R-EBUS status and Reposition (Improved/Unimproved)

Reposition Outcome	Initial Within (n = 242)	Initial Adjacent (n = 108)	Initial Invisible (n = 13)
Improved	—	38 / 50 (76.0%)	2 / 2 (100%)
Unimproved	—	31 / 58 (53.5%)	1 / 11 (9.1%)
Total Yield	199 / 242 (82.2%)	69 / 108 (63.9%)	3 / 13 (23.1%)

R-EBUS, radial endobronchial ultrasound

Table 3 Multivariable logistic regression analysis of R-EBUS image improvement on diagnostic yield

Variables	Reference	OR	95% CI	p
R-EBUS image, improved	unimproved	3.55	1.57–8.06	0.002
Size, > 20 mm	≤ 20 mm	1.50	0.67–3.36	0.320
Location, inner	outer	1.24	0.56–2.74	0.589
CT bronchus sign, positive	negative	1.02	0.43–2.41	0.968

R-EBUS, radial endobronchial ultrasound; CT, computed tomography; OR, odds ratio; CI, confidence interval

Diagnostic yield did not differ significantly between TBOnly (73.6 %) and combined TBNA + TBB (78.3 %) in the overall cohort ($p=0.38$). However, in lesions that were initially adjacent, adding TBNA increased yield from 52.9 % to 73.7 % ($p=0.019$). In malignant lesions ($n=303$), sensitivity followed the same pattern: 84.7 % for the initialwithin group, 68.5% for lesions initially adjacent, and 33.3% for lesions initially invisible (Supplementary Table S1). Among lesions not initially within, sensitivity improved from 54.7 to 77.1% when the probe–lesion relation was upgraded ($p=0.022$).

Multivariable logistic regression analysis

The impact of improved R-EBUS findings on diagnostic yield was evaluated using multivariable logistic regression analysis, adjusted for lesion size (dichotomized at 20 mm), lesion location, and bronchus sign on CT. The multivariable logistic regression model revealed that the OR for intraoperative improvement in R-EBUS findings was 3.55 (95% CI: 1.57–8.06, $p=0.002$), indicating a statistically significant effect (Table 3). A parallel model in malignant lesions yielded a comparable adjusted OR of 2.62 (95% CI 1.09–6.32).

SHAP beeswarm plot analysis

In patients whose initial R-EBUS images were not “within,” a random forest model was constructed to predict improved probe–lesion positioning. The SHAP beeswarm plot (Fig. 3) revealed that lesion location was the most influential predictor, with inner lesions associated with a higher likelihood of improvement. Radiographic visibility showed a modest positive effect; visible lesions were slightly more likely to yield successful repositioning, whereas non-visible lesions tended to be associated with negative SHAP values and greater variability. Lesion size exhibited a mosaic-like distribution of SHAP values, indicating that size alone was not a decisive

predictor. Similarly, the CT bronchus sign displayed a mosaic pattern, suggesting that it was not a strong determinant. For lesion structure, the SHAP values for solid lesions were concentrated near zero, while subsolid lesions tended to be more variable.

Complications

The incidence of complications was low across all groups. As shown in Table 4, the improved R-EBUS image group had a total complication rate of 5.8%, whereas the unimproved R-EBUS image group had a rate of 4.3%. The total complication rate in the initially within-group was 6.2%. The most common complication was pneumothorax, occurring in 1.9% of patients in the improved R-EBUS image group, 2.9% in the unimproved R-EBUS image group, and 2.9% in the initially within-group. Infection occurred in 3.8% of patients in the improved R-EBUS image group and 2.9% of patients in the initially within-group but was not observed in the unimproved R-EBUS image group. Haemorrhage requiring a haemostatic agent was rare, occurring in only 0.4% of patients in the initially within-group and none in the other groups. No statistically significant differences in complication rates were observed between the groups ($p>0.05$).

Discussion

In this retrospective analysis of 363 patients with PPLs undergoing TBNA and/or transbronchial biopsy (TBB) with endobronchial ultrasonography using a guide sheath (EBUS-GS), we investigated whether intraoperative improvement in R-EBUS imaging could enhance the diagnostic yield without increasing complications. Our main finding was that lesions in which the R-EBUS probe–lesion relation improved intraoperatively had a significantly higher diagnostic yield (76.9%) than that of those in which improvement did not occur (46.4%). Multivariable regression analysis further underscored that this improvement independently predicted a high diagnostic yield (adjusted OR: 3.55, 95% CI: 1.57–8.06). When the probe–lesion relation remained invisible despite careful repositioning, the diagnostic yield fell to 9.1%. In such instances, further bronchoscopic sampling is unlikely to be informative, and early referral for CT-guided percutaneous biopsy may therefore be considered to avoid diagnostic delay. Furthermore, our exploratory machine-learning analysis (random-forest model with

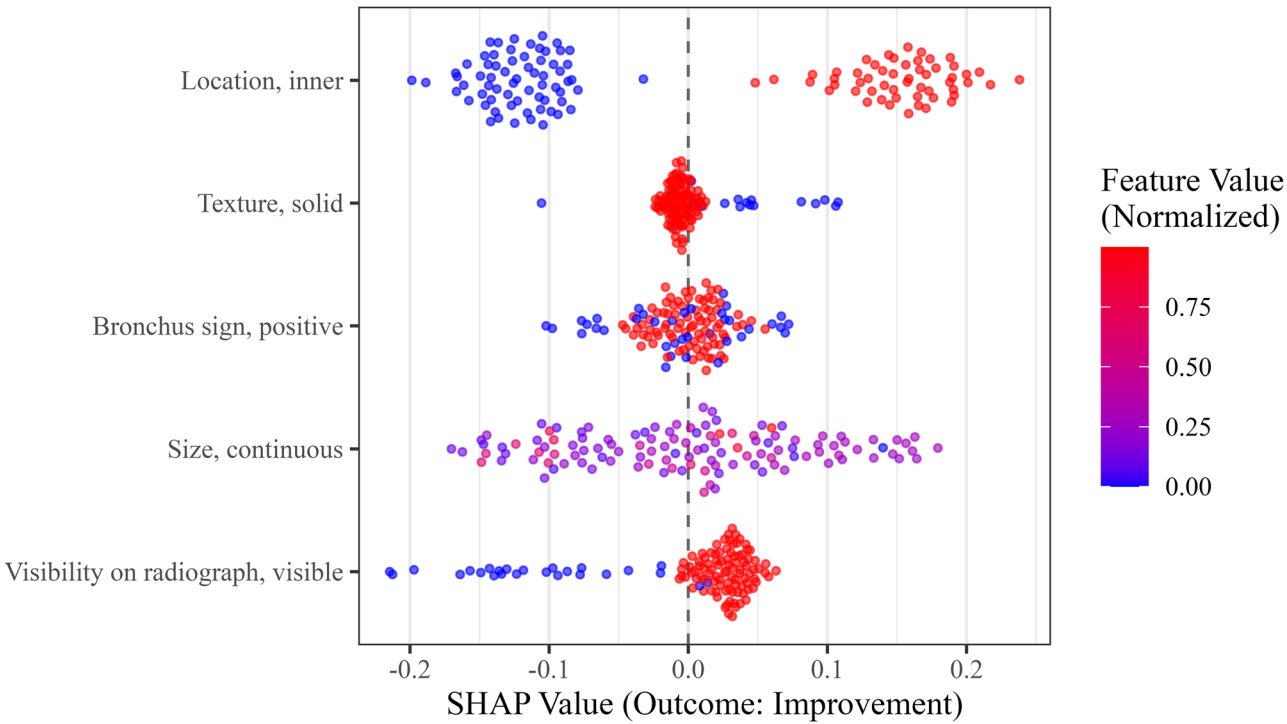


Fig. 3 SHAP Beeswarm Plot of Predictors for Improved R-EBUS Imaging. A SHAP beeswarm plot illustrating the impact of each feature on the prediction of successful intraoperative improvement in R-EBUS imaging using a random forest model. Each dot represents a single patient case. The x-axis indicates the SHAP value, which reflects the contribution of that feature to the model output (positive values increase the likelihood of improvement). Dot colors represent normalized feature values (red = high, blue = low). Lesion location showed a relatively clear positive impact, with inner lesions associated with greater likelihood of successful repositioning. Radiographic visibility also demonstrated a moderate positive effect. In contrast, features such as bronchus sign and lesion size exhibited more variable, mosaic-like SHAP distributions, indicating a less consistent predictive influence. The lesion structure (“solid”) feature showed minimal overall contribution, with SHAP values centered near zero

Table 4 Comparison of complications across R-EBUS image status groups

Complication	Improved EBUS Image Group (n = 52)	Unimproved EBUS Image Group (n = 69)	Initially Within Group (n = 242)	p
Pneumothorax (%)	1 (1.9)	2 (2.9)	7 (2.9)	> 0.999
Infection (%)	2 (3.8)	0 (0)	7 (2.9)	0.296
Haemorrhage (%)	0 (0)	0 (0)	1 (0.4)	> 0.999
Other Complications (%)	0 (0)	1 (1.4)	2 (0.8)	0.705
Total Complications (%)	3 (5.8)	3 (4.3)	15 (6.2)	0.943

R-EBUS, radial endobronchial ultrasound

SHAP) showed that inner lesion location was the most robust predictor, whereas radiographic visibility made a modest positive contribution that emerged only after accounting for lesion size, bronchus sign, and anatomical depth; visibility should therefore be regarded as one of several interacting factors, rather than a stand-alone determinant, when judging the likelihood of successful probe repositioning. Importantly, complication rates remained low and did not differ significantly among the improved, unimproved, and initially within-groups, suggesting that repeated attempts to optimize probe positioning did not introduce additional procedural risk.

Our findings align with and add detail to prior studies emphasizing that the “within” position of the ultrasound

probe is crucial for maximizing the diagnostic yield. Previous reports have shown diagnostic yields of 80 to 90% when the R-EBUS probe is within the lesion, whereas yields drop substantially when the probe is only adjacent or invisible [6–8]. Yamada et al. [7] demonstrated that the diagnostic yield was 83% when the probe was “within,” 61% when “adjacent,” and only 4% when “outside.” Similarly, meta-analyses have reported pooled yields of 70 to 72% for R-EBUS-guided TBB, highlighting the importance of achieving and maintaining an optimal probe–lesion relation [6].

In our study, the initially within-group had an 82.2% diagnostic yield, consistent with these prior reports, whereas lesions that were initially adjacent or invisible

fared worse unless further manoeuvres allowed more advantageous probe repositioning. This underscores how active intraoperative adjustments can partially compensate for initially suboptimal ultrasound views.

Our overall complication rates (4–6%) compared favourably with prior work on R-EBUS-guided biopsy procedures, which reported pneumothorax rates ranging from 1% to approximately 5% and serious bleeding in less than 1–2% of cases [6, 17]. In line with these data, we observed no statistically significant difference in complication rates across the unimproved, improved, and initially within-groups, with pneumothorax occurring in approximately 2–3% of patients in each group. These findings suggest that additional sampling manoeuvres—such as repeated probe insertion or minor repositioning to enhance EBUS images—can be performed safely.

Yamamoto et al. investigated predictive factors for the transition of R-EBUS findings from “adjacent to” to “within” in EBUS-GS and identified larger lesion diameter (≥ 29.25 mm) as a key driver of successful repositioning, suggesting that bigger lesions enable deeper probe advancement to reach an intralesional position [21]. In contrast, our additional random forest model and SHAP analysis showed that lesion location (inner vs. outer) emerged as a more consistent determinant of improved R-EBUS positioning than lesion diameter, and that radiographic visibility also had a positive—though milder—effect. This discrepancy may stem from methodological differences: while Yamamoto et al. focused on TBB alone, our study incorporated both TBB and TBNA, thereby expanding the scope of sampling maneuvers and potentially diminishing the impact of lesion size as a single predictor. Indeed, our SHAP-based approach revealed a mosaic-like influence of lesion diameter and bronchus sign, indicating their variable contribution under different clinical contexts. Despite these nuanced differences, both studies highlight the fundamental principle that deliberate, repeated probe repositioning can significantly optimize diagnostic yield when R-EBUS images initially show only an “adjacent to” position. By combining traditional risk stratification (e.g., lesion size) with broader factors such as lesion location and visibility—along with adjunct techniques like TBNA—clinicians can be more targeted in deciding whether additional time spent repositioning the probe is worthwhile.

Our findings further complement those reported by Ito et al., [12] who demonstrated that the addition of TBNA to TBB with EBUS-GS improves diagnostic performance. In contrast to that study, which focused primarily on the incremental benefit of adding TBNA, our analysis uniquely emphasized the value of deliberate intraoperative enhancements in R-EBUS imaging. Although our patient populations overlapped, our study specifically investigated the quantitative impact of improved imaging

on diagnostic yield, thereby offering complementary insights rather than redundant findings.

In our cohort, adding TBNA to TBB increased diagnostic yield from 74 to 78% overall and—from 53–74%—in lesions that were initially adjacent. Alternative and adjunctive sampling techniques have also been proposed for lesions that remain “adjacent” on radial-EBUS. Transbronchial cryobiopsy can yield diagnostic accuracies of 85–95% while providing larger transmural specimens, but mild to moderate bleeding occurs in approximately 20–30% of cases [22]. Robot-assisted bronchoscopy (RAB) achieves yields of 69–77% with pneumothorax and significant bleeding each occurring in $<4\%$, a safety profile comparable to conventional radial-EBUS but at the cost of substantial capital investment and the frequent need for general anaesthesia [23]. A recent decision-analytic model estimates that every 10-percentage-point increase in bronchoscopic sensitivity confers a net monetary benefit of about US \$8 700 per patient by accelerating diagnosis and treatment [24]. Given that both cryobiopsy and RAB involve higher disposable or infrastructure costs, their routine use is justified only when a clear diagnostic advantage is anticipated. More widely available adjuncts—such as cytology brushing, catheter aspiration, and cell-block preparation from guide-sheath rinse fluid—can provide incremental yield when histology alone is insufficient. Selection among these modalities should therefore be individualised, balancing expected gains in sensitivity against bleeding risk, anaesthetic requirements, and local resource constraints.

This study had several limitations. First, this was a retrospective single-centre study with a relatively small sample size, which may limit the generalizability, and unmeasured confounding variables may have influenced our results. Second, classification of radial-EBUS images is partly subjective, and some inter-observer variability cannot be excluded [25]. Third, although the outcomes evaluated in this study—diagnostic yield and safety—are critical for assessing the quality of bronchoscopic procedures; however, these alone may not fully capture healthcare quality. Fourth, procedure duration could not be compared because start–end times were not captured in the original data collection. Fifth, we did not record an objective measure of airway complexity (e.g. the number of bronchial divisions beyond the visual field), which could have biased diagnostic yield toward more easily accessible lesions [26]. Sixth, we did not prospectively determine whether biopsy specimens provided sufficient cellularity or nucleic-acid yield for comprehensive genomic testing; future studies should include predefined metrics of molecular adequacy [27, 28]. Efforts aimed at improving probe positioning and R-EBUS imaging can enhance diagnostic accuracy but may also extend procedural duration [29] and increase patient discomfort

or anxiety [30]. Therefore, a more comprehensive evaluation—including these additional factors—is necessary to better understand the overall impact of intraoperative strategies designed to improve diagnostic performance, ultimately contributing to a more holistic improvement in healthcare quality. Further research, including larger prospective studies, is required to confirm and extend our findings.

Conclusions

Improved R-EBUS findings during TBNA/TBB or TBB with EBUS-GS were associated with a high diagnostic yield, even when the initial R-EBUS findings were inadequate. Moreover, our machine learning analysis highlighted that an inner lesion location and radiographic visibility are key predictors of successful probe repositioning, offering additional guidance on when repeated maneuvers may be most beneficial. Taken together, these results suggest that combining TBNA with TBB, in addition to performing TBB during EBUS-GS, to enhance R-EBUS imaging during bronchoscopy may be a valuable strategy for increasing the probability of achieving a higher diagnostic yield.

Supplementary Information

The online version contains supplementary material available at <https://doi.org/10.1186/s12890-025-03725-7>.

Supplementary Material 1

Supplementary Material 2

Acknowledgements

We thank Editage for English language editing.

Author contributions

KN conceived the concept, conducted the statistical analyses, and led manuscript drafting. TI designed the study, coordinated data collection, managed ethical approval processes, and supervised the statistical review and manuscript preparation. SI provided guidance on imaging diagnostics, clinical suggestions, and manuscript comments. SO, SN, and TFCY contributed clinical oversight, supplemental information, and manuscript feedback. BC supplemented the statistical analysis review, refined the manuscript, and provided interpretative comments. MI served as the overall leader, overseeing the entire study. All authors reviewed and approved the final manuscript.

Funding

None.

Data availability

The data supporting the findings of this study are not publicly available because of privacy and ethical restrictions related to patient confidentiality. However, the data are available from the corresponding author upon reasonable request and approval from the Institutional Review Board of Nagoya University Hospital.

Declarations

Ethics approval and consent to participate

This retrospective observational study was approved by the Institutional Review Board of Nagoya University Hospital (approval number: 2022–0158). As the study design is observational, registration details such as a trial

registration number, registry, and registration date are not applicable. The requirement for individual patient consent was waived due to the retrospective nature of the data collection and analysis. All patient-related information was anonymized prior to use. The study was conducted in accordance with the principles of the Declaration of Helsinki.

Consent for publication

Consent for publication of anonymized data was not deemed necessary by the Institutional Review Board under the approved protocol. Any images included in this manuscript have been de-identified in compliance with local privacy regulations.

Competing interests

The authors declare no competing interests.

Author details

¹Department of Advanced Medicine, Nagoya University Hospital, Nagoya, Japan

²Department of Biostatistics, Kyoto University School of Public Health, Kyoto, Japan

³Department of Respiratory Medicine, Nagoya University Graduate School of Medicine, Nagoya, Japan

⁴Department of Radiology, Nagoya University Graduate School of Medicine, Nagoya, Japan

⁵Department of Respiratory Medicine, Fujita Health University School of Medicine, Aichi, Japan

⁶Department of Thoracic Surgery, Nagoya University Graduate School of Medicine, Nagoya, Japan

⁷Department of International Medical Education, Nagoya University Graduate School of Medicine, Nagoya, Japan

Received: 5 April 2025 / Accepted: 13 May 2025

Published online: 26 May 2025

References

1. National Lung Screening Trial, Research T, Aberle DR, Adams AM, Berg CD, Black WC, Clapp JD, Fagerstrom RM, Gareen IF, Gatsonis C, Marcus PM, et al. Reduced lung-cancer mortality with low-dose computed tomographic screening. *N Engl J Med*. 2011;365(5):395–409.
2. Silvestri GA, Gonzalez AV, Jantz MA, Margolis ML, Gould MK, Tanoue LT, Harris LJ, Detterbeck FC. Methods for staging non-small cell lung cancer: diagnosis and management of lung cancer, 3rd ed: American college of chest physicians evidence-based clinical practice guidelines. *Chest*. 2013;143(5 Suppl):eS211–50.
3. Gould MK, Fletcher J, Iannettoni MD, Lynch WR, Midthun DE, Naidich DP, Ost DE, American College of Chest P: Evaluation of patients with pulmonary nodules: when is it lung cancer? ACCP evidence-based clinical practice guidelines (2nd edition). *Chest*. 2007;132(3 Suppl):108S–130S.
4. Ali MS, Trick W, Mba BI, Mohanane D, Sethi J, Musani AI. Radial endobronchial ultrasound for the diagnosis of peripheral pulmonary lesions: A systematic review and meta-analysis. *Respirology*. 2017;22(3):443–53.
5. Eberhardt R, Anantham D, Ernst A, Feller-Kopman D, Herth F. Multimodality bronchoscopic diagnosis of peripheral lung lesions: a randomized controlled trial. *Am J Respir Crit Care Med*. 2007;176(1):36–41.
6. Kim SH, Chung HS, Kim J, Kim MH, Lee MK, Kim I, Eom JS. Development of the Korean association for lung Cancer clinical practice guidelines: recommendations on radial probe endobronchial ultrasound for diagnosing lung Cancer - An updated Meta-Analysis. *Cancer Res Treat*. 2024;56(2):464–83.
7. Yamada N, Yamazaki K, Kurimoto N, Asahina H, Kikuchi E, Shinagawa N, Oizumi S, Nishimura M. Factors related to diagnostic yield of transbronchial biopsy using endobronchial ultrasonography with a guide sheath in small peripheral pulmonary lesions. *Chest*. 2007;132(2):603–8.
8. Kurimoto N, Miyazawa T, Okimasa S, Maeda A, Oiwa H, Miyazu Y, Murayama M. Endobronchial ultrasonography using a guide sheath increases the ability to diagnose peripheral pulmonary lesions endoscopically. *Chest*. 2004;126(3):959–65.
9. Guven C, Yserbyt J, Testelmans D, Zanca F, Carbonez A, Ninane V, De Wever W, Dooms C. Computed tomography characteristics predictive for radial EBUS-miniprobe-guided diagnosis of pulmonary lesions. *J Thorac Oncol*. 2015;10(3):472–8.

10. Izumo T, Sasada S, Chavez C, Matsumoto Y, Tsuchida T. Radial endobronchial ultrasound images for ground-glass opacity pulmonary lesions. *Eur Respir J*. 2015;45(6):1661–8.
11. Nakajima T, Yasufuku K, Takahashi R, Shingyoji M, Hirata T, Itami M, Matsui Y, Itakura M, Iizasa T, Kimura H. Comparison of 21-gauge and 22-gauge aspiration needle during endobronchial ultrasound-guided transbronchial needle aspiration. *Respirology*. 2011;16(1):90–4.
12. Ito T, Nishida K, Iwano S, Okachi S, Nakamura S, Morise M, Chen-Yoshikawa T, Ishii M. Diagnostic value and safety of addition of transbronchial needle aspiration to transbronchial biopsy through endobronchial ultrasonography using a guide sheath under virtual bronchoscopic navigation for the diagnosis of peripheral pulmonary lesions. *J Bronchol Interv Pulmonol* 2024;31(4).
13. Shinagawa N, Takashima Y, Kashima M, Morinaga D, Ito S, Tsuji K, Sato M, Takahashi H, Shoji T, Furuta M et al. Evaluating the usefulness of the insertion tube rotation function of bronchoscope in cadaver models. *J Bronchol Interv Pulmonol* 2025;32(2).
14. Hayama M, Izumo T, Chavez C, Matsumoto Y, Tsuchida T, Sasada S. Additional transbronchial needle aspiration through a guide sheath for peripheral pulmonary lesions that cannot be detected by radial EBUS. *Clin Respir J*. 2017;11(6):757–64.
15. Matsumoto Y, Izumo T, Sasada S, Tsuchida T, Ohe Y. Diagnostic utility of endobronchial ultrasound with a guide sheath under the computed tomography workstation (ziostation) for small peripheral pulmonary lesions. *Clin Respir J*. 2017;11(2):185–92.
16. Kim H, Park CM, Koh JM, Lee SM, Goo JM. Pulmonary sub-solid nodules: what radiologists need to know about the imaging features and management strategy. *Diagn Interv Radiol*. 2014;20(1):47–57.
17. Asano F, Aoe M, Ohsaki Y, Okada Y, Sasada S, Sato S, Suzuki E, Senba H, Fujino S, Ohmori K. Deaths and complications associated with respiratory endoscopy: a survey by the Japan society for respiratory endoscopy in 2010. *Respirology*. 2012;17(3):478–85.
18. Ponce-Bobadilla AV, Schmitt V, Maier CS, Mensing S, Stodtmann S. Practical guide to SHAP analysis: explaining supervised machine learning model predictions in drug development. *Clin Transl Sci*. 2024;17(11):e70056.
19. Lundberg SM, Lee S-I. A unified approach to interpreting model predictions. In: *Proceedings of the 31st international conference on neural information processing systems*. Long Beach, California, USA: Curran Associates Inc. 2017, pp. 4768–4777.
20. Uematsu T, Tsuboi T, Hiraga K, Tamakoshi D, Fukushima T, Sato M, Nishida K, Yokota H, Katsuno M. Differential impact of fixation characteristics on 3D perception via texture gradient recognition in Parkinson's disease. *Parkinsonism Relat Disord*. 2024;128:107116.
21. Yamamoto S, Matsui H, Fujioka H, Homma Y, Kubota N, Otsuki A, Ito H, Sagara H, Nakashima K. Predictors of improvement of radial-endobronchial ultrasonography findings from adjacent to to within in endobronchial ultrasonography using a guide sheath: a retrospective cohort study. *J Thorac Dis*. 2024;16(1):264–72.
22. Sryma PB, Mittal S, Madan NK, Tiwari P, Hadda V, Mohan A, Guleria R, Madan K: Efficacy of Radial Endobronchial Ultrasound (R-EBUS) guided transbronchial cryobiopsy for peripheral pulmonary lesions (PPL... s): A systematic review and meta-analysis. *Pulmonology* 2023;29(1):50–64.
23. Chaddha U, Kovacs SP, Manley C, Hogarth DK, Cumbo-Nacheli G, Bhavani SV, Kumar R, Shende M, Egan JP 3rd, Murgu S. Robot-assisted bronchoscopy for pulmonary lesion diagnosis: results from the initial multicenter experience. *BMC Pulm Med*. 2019;19(1):243.
24. Ost DE, Maldonado F, Shafrin J, Kim J, Marin MA, Amos TB, Hertz DS, Kalsekar I, Vachani A. Economic value of bronchoscopy technologies that improves sensitivity for malignancy for peripheral pulmonary lesions. *Ann Am Thorac Soc*. 2024;21(12):1759–69.
25. Kurimoto N, Murayama M, Yoshioka S, Nishisaka T. Analysis of the internal structure of peripheral pulmonary lesions using endobronchial ultrasonography. *Chest*. 2002;122(6):1887–94.
26. Roth K, Eagan TM, Andreassen AH, Leh F, Hardie JA. A randomised trial of endobronchial ultrasound guided sampling in peripheral lung lesions. *Lung Cancer*. 2011;74(2):219–25.
27. Sakaguchi T, Nishii Y, Iketani A, Esumi S, Esumi M, Furuhashi K, Nakamura Y, Suzuki Y, Ito K, Fujiwara K, et al. Comparison of the analytical performance of the Oncomine Dx target test focusing on bronchoscopic biopsy forceps size in non-small cell lung cancer. *Thorac Cancer*. 2022;13(10):1449–56.
28. Naso J, Bras J, Villamil C, Ionescu DN, Wang G, Shaipanich T, Beaudoin EL, Myers R, Lam S, Zhou C. Cytologic features and diagnostic value of PeriView FLEX transbronchial needle aspiration targeting pulmonary nodules. *Cancer Cytopathol*. 2020;128(5):333–40.
29. Kim EJ, Kim KC. Utility of radial probe endobronchial Ultrasound-Guided transbronchial lung biopsy in diffuse lung lesions. *Tuberc Respir Dis (Seoul)*. 2019;82(3):201–10.
30. Yildirim F, Ozkaya S, Yurdakul AS. Factors affecting patients' comfort during fiberoptic bronchoscopy and endobronchial ultrasound. *J Pain Res*. 2017;10:775–81.

Publisher's note

Springer Nature remains neutral with regard to jurisdictional claims in published maps and institutional affiliations.